J|A|C|S
ARTICLES
Published on Web 09/20/2002

How Ions Affect the Structure of Water

Barbara Hribar,[†] Noel T. Southall,[‡] Vojko Vlachy,[†] and Ken A. Dill*[,§]

Contribution from the Faculty of Chemistry and Chemical Technology, University of Ljubljana, Askerčeva 5, 1000 Ljubljana, Slovenia, Graduate Group in Biophysics, University of California, San Francisco, California 94143-1204, and Department of Pharmaceutical Chemistry and Graduate Group in Biophysics, University of California, San Francisco, California 94143-1204

Received February 23, 2002

Abstract: We model ion solvation in water. We use the MB model of water, a simple two-dimensional statistical mechanical model in which waters are represented as Lennard-Jones disks having Gaussian hydrogen-bonding arms. We introduce a charge dipole into MB waters. We perform (NPT) Monte Carlo simulations to explore how water molecules are organized around ions and around nonpolar solutes in salt solutions. The model gives good qualitative agreement with experiments, including Jones−Dole viscosity *B* coefficients, Samoilov and Hirata ion hydration activation energies, ion solvation thermodynamics, and Setschenow coefficients for Hofmeister series ions, which describe the salt concentration dependence of the solubilities of hydrophobic solutes. The two main ideas captured here are (1) that charge densities govern the interactions of ions with water, and (2) that a balance of forces determines water structure: electrostatics (water's dipole interacting with ions) and hydrogen bonding (water interacting with neighboring waters). Small ions (kosmotropes) have high charge densities so they cause strong electrostatic ordering of nearby waters, breaking hydrogen bonds. In contrast, large ions (chaotropes) have low charge densities, and surrounding water molecules are largely hydrogen bonded.

1. Introduction

Ion−water interactions are important throughout biology and chemistry. Ions affect the conformations and activities of proteins and nucleic acids[1−3] and the specificity of ion binding. Ion complexation in cells is crucial for the activities of biomolecules such as enzymes and drugs.[4,5] Ions regulate the electrostatic potentials, conductances, and permeabilities of cell membranes,[6,7] the structures of micelles, and the hydrophobic effect (called Hofmeister effects), which drives partitioning, permeation, and folding and binding processes.[8,9] In chemistry, ions affect the rates of chemical reactions;[10,11] rates of gelation, widely used in food applications;[12] ion-exchange mechanisms, widely used for chemical separations;[13] and the expansion and contraction of clays, responsible for environmental processes such as mudslides.[14] Ion hydration has been studied extensively, both experimentally[15−19] and theoretically.[20−25]

Ions have long been classified as being either kosmotropes (structure makers) or chaotropes (structure breakers) according to their relative abilities to induce the structuring of water. The degree of water structuring is determined mainly by two types of quantities: the increase or decrease in viscosity in water due to added salt, and entropies of ion solvation. For example, the viscosity η of an aqueous salt solution typically has the following dependence on ion concentration c:[18]

$$\eta/\eta_0 = 1 + Ac^{1/2} + Bc + ... \quad (1)$$

where η_0 is the viscosity of pure water at the same temperature.

* To whom correspondence should be addressed. E-mail: dill@zimm.ucsf.edu.
[†] University of Ljubljana.
[‡] Graduate Group in Biophysics, University of California.
[§] Department of Pharmaceutical Chemistry and Graduate Group in Biophysics, University of California.

(1) Dill, K. A. *Biochemistry* **1990**, *29*, 7133−7155.
(2) Rupley, J.; Careri, G. *Adv. Protein Chem.* **1991**, *41*, 37−172.
(3) Chalikian, T. V.; Volker, J.; Plum, E.; Breslauer, K. *Proc. Natl. Acad. Sci. U.S.A.* **1999**, *96*, 7853−7858.
(4) Sussman, F.; Weinstein, H. *Proc. Natl. Acad. Sci. U.S.A.* **1989**, *86*, 7880−7884.
(5) Lybrand, T. P.; McCammon, A.; Wiff, G. *Proc. Natl. Acad. Sci. U.S.A.* **1986**, *83*, 833−835.
(6) Jordan, P. C. *Biophys. J.* **1990**, *58*, 1133−1156.
(7) Katz, B. *Nerve, Muscle, and Synapse*; McGraw-Hill: London, 1966.
(8) Collins, K. D.; Washabaugh, M. W. *Q. Rev. Biophys.* **1985**, *18*, 323−422.
(9) Cacace, M. G.; Landau, E. M.; Ramsden, J. J. *Q. Rev. Biophys.* **1997**, *30*, 241−277.
(10) Maroncelli, M.; MacInnins, J.; Fleming, G. R. *Science* **1989**, *243*, 1674−1681.
(11) Kropman, M. F.; Bakker, H. J. *Science* **2001**, *291*, 2118−2120.
(12) Larwood, V. L.; Howlin, B. J.; Webb, G. A. *J. Mol. Model.* **1996**, *2*, 175−
(13) Habuchi, S.; Kim, H. B.; Kitamura, N. *Anal. Chem.* **2001**, *73*, 366−372.
(14) Chavez-Paez, M.; Van Workum, K.; de Pablo, L.; de Pablo, L. L. *J. Chem. Phys.* **2001**, *114*, 1405−1413.
(15) Samoilov, O. Y. *Discuss. Faraday Soc.* **1957**, *24*, 141−146.
(16) Samoilov, O. Y. In *Water and Aqueous Solution: Structure, Thermodynamics, and Transport Processes*; Horne, R. A., Ed.; Wiley-Interscience: New York, 1972; pp 597−612.
(17) Krestov, G. A. *Thermodynamics of Solvation*; Ellis Horwood: New York, 1990.
(18) Robinson, R. A.; Stokes, R. H. *Electrolyte Solutions*; Butterworth Scientific Publications: London, 1959.
(19) Bernal, J. D.; Fowler, R. H. *J. Chem. Phys.* **1933**, *1*, 515−548.
(20) Marx, D.; Sprik, M.; Sprik, M.; Parinello, M. *Chem. Phys. Lett.* **1997**, *273*, 360−366 and references therein.
(21) Heinzinger, K.; Vogel, P. C. *Z. Naturforsch.* **1974**, *A29*, 1164−1171.
(22) Galli, G.; Parrinello, M. In *Computer Simulations in Materials Science*; Meyer, M., Pontikis, V., Eds.; Kluwer: Dordrecht, 1991.
(23) Payne, M. C.; Teter, M. P.; Allan, D. C.; Arias, T. A.; Joannopoulos, J. D. *Rev. Mod. Phys.* **1992**, *64*, 1045−1097.
(24) Galli, G.; Pasquarello, A. In *Computer Simulations in Chemical Physics*; Allen, M. P., Tildesley, D. J., Eds.; Kluwer: Dordrecht, 1993.
(25) Hummer, G.; Pratt, L. R.; Garcia, A. E. *J. Phys. Chem. A* **1998**, *102*, 7885−

A is a constant independent of c; its corresponding term can be explained by Debye−Hückel theory as being due to counterion screening at low ion concentrations. The constant B, which is called the Jones−Dole B coefficient, is the quantity that defines the degree of water structuring of interest here.[18] B is positive for kosmotropic ions and negative for chaotropic ions. One issue in interpreting experiments is how to separate the contributions of the anion from the cation. The standard assumption is that K^+ has the same B coefficient as Cl^-, $B_{K^+} = B_{Cl^-}$, because K^+ and Cl^- have approximately the same ionic conductances[26] and because the value of B for KCl is approximately zero.

Water structuring is also reflected in entropies of ion solvation. To obtain these entropies, two assumptions are commonly used. First, to separate the effects of the anion from the cation, it is assumed that the solvation entropies are additive.[17] Second, an assumption is required to parse the ion solvation entropy into components due to the ion and due to water. By splitting the solvation entropy, ΔS^{hyd}, into ion and hydration water contributions and subtracting the former, ΔS_{II} is obtained, which describes the change in entropy of hydration water due to the presence of an ion.[17] Ions which are kosmotropic in viscosity experiments tend to have a negative hydration component to their solvation entropy, implying that they order the nearby waters, while chaotropic ions have a positive ΔS_{II}.

The experiments show that water is ordered by small or multivalent ions and disordered by large monovalent ions. Therefore, water ordering has generally been interpreted in terms of ion charge densities.[17,27] Charge densities are high on ions that have a small radius and/or a large charge.

A related property is the Hofmeister effect.[28] In 1888, Hofmeister reported that salts affect the solubilities of proteins in water to varying degrees. This has been interpreted as a modulation of the hydrophobic effect by salts because it is also found that increasing salt concentration reduces the solubilities of simple hydrophobic solutes such as benzene in aqueous solutions.[29,30] The Hofmeister series is a list of ions rank-ordered in terms of how strongly they modulate hydrophobicity. Such salt effects on nonpolar solubilities correlate with charge densities of the salts. Small ions tend to cause "salting out", that is, to reduce hydrophobic solubilities in water, whereas large ions tend to cause "salting-in", increasing nonpolar solubilities. The Hofmeister series, however, does not correlate perfectly with ionic charge density: while lithium is smaller than sodium, lithium has a weaker Hofmeister effect.

The Hofmeister effect is directly proportional to salt concentration and modeled by the Setschenow equation:[31]

$$\ln[c_i/c_i(0)] = -k_s c_s \qquad (2)$$

where c_i and $c_i(0)$ are the molar solubilities of the hydrophobe in a salt solution and water, respectively, c_s is the molar concentration of the salt, and k_s is the salt's Setschenow salting-out coefficient.

There are various microscopic perspectives on these properties. Smith[32] and Kalra et al.[33] have calculated Setschenow coefficients from molecular dynamics simulations. In their simulations, the hydrophobe−ion pair distribution functions show that strongly salting-out (small) ions are generally excluded from the nonpolar solute's first water shell.

In 1957, Samoilov[15,16] proposed that dynamic properties, such as the viscosity, could be understood in terms of the activation energy required to strip a water molecule away from the first solvation shell of an ion as compared to that for another water, $\Delta E_i = E_i - E_0$. E_0 is the activation energy for the process of transferring a water molecule from a first shell around another water molecule to its next coordination shell, and E_i is the corresponding activation energy for a water molecule in an ion coordination shell.[15] A water molecule "binds" to a small ion more tightly than it binds to a neighboring water molecule, resulting in a positive activation energy, while water molecules next to big ions are more mobile than bulk water molecules ($\Delta E_i < 0$).

Collins[27] proposed that ion effects on water structure could be explained by a competition between ion−water interactions, which are dominated by charge density effects, and water−water interactions, which are dominated by hydrogen bonding. He explained that anions are stronger than cations at water ordering because of the asymmetry of charge in a water molecule: the negative end of water's dipole is nearer to the center of the water molecule than the positive end. Therefore, anions see a larger electrostatic potential at the surface of a water molecule than cations see. Our preliminary calculations indicate[34] that the solvation model of Collins yields qualitative agreement with the experimental data. We were motivated by Collins' insightful qualitative model to make a more quantitative statistical mechanical model.

2. The Model and Simulation

We wanted a model that (1) is physical, that is, based on an energy function related to the structure of water, and (2) is computationally efficient enough to sample the spatial and energetic distributions of water molecules. High-resolution all-atom simulations are computationally intensive, particularly for studies, such as Hofmeister effects, that involve three species: water, ion, and nonpolar solute. Here we use the MB model, in which each water molecule is represented as a two-dimensional disk that interacts with other waters through a Lennard-Jones (LJ) interaction and through an orientation-dependent hydrogen-bonding (HB) interaction. The name "MB" arises because there are three hydrogen-bonding arms, arranged as in the Mercedes Benz logo (Figure 1). There are various anomalous properties of pure water[35−39] including the density anomaly, a minimum in isothermal compressibility, and a large heat capacity; they are reproduced qualitatively by the MB model.[40] The model

(26) Kaminsky, M. *Discuss. Faraday Soc.* **1957**, *24*, 171−179.
(27) Collins, K. D. *Biophys. J.* **1997**, *72*, 65−76.
(28) Hofmeister, F. *Arch. Exp. Pathol. Pharmakol.* **1888**, *24*, 247−260.
(29) McDevit, W. F.; Long, F. A. *J. Am. Chem. Soc.* **1952**, *74*, 1773−1777.
(30) von Hippel, P. H.; Schleich, T. *Acc. Chem. Res.* **1969**, *2*, 257−265.
(31) Baldwin, R. L. *Biophys. J.* **1996**, *71*, 2056−2063.
(33) Kalra, A.; Tugcu, N.; Cramer, S.; Garde, S. *J. Phys. Chem. B* **2001**, *105*, 6380−6386.
(34) Kalyuzhnyi, Yu. V.; Vlachy, V.; Dill, K. *Acta Chim. Slov.* **2001**, *48*, 309−316.
(35) Eisenberg, D.; Kauzmann, W. *The Structure and Properties of Water*; Oxford University Press: Oxford, 1969.
(36) Franks, F., Ed. *Water, A Comprehensive Treatise*; Plenum Press: New York, 1972−1982; Vols. 1−7.
(37) Stillinger, F. H. *Science* **1980**, *209*, 451−457.
(38) Zhu, S. B.; Singh, S.; Robinson, G. W. *Adv. Chem. Phys.* **1994**, *85*, 627−731.
(39) Robinson, G.; Zhu, S. B.; Singh, S.; Evans, M. *Water in Biology, Chemistry, and Physics: Experimental Overviews and Computational Methodologies*; World Scientific: Singapore, 1996.
(40) Silverstein, K. A.; Haymet, A. D. J.; Dill, K. A. *J. Am. Chem. Soc.* **1998**,

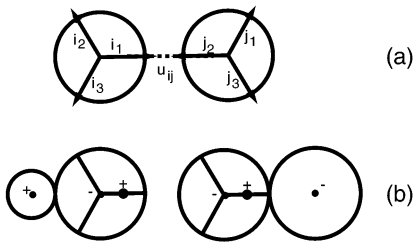

Figure 1. The MB-dipole model. (a) Two MB-dipole waters forming a hydrogen bond. (b) A cation and an MB-dipole water oriented in its most favorable orientation (180° with respect to the vector connecting the molecular centers). Also an anion and a water oriented in its most favorable orientation (0°).

also captures qualitatively the properties of the water as a solvent for nonpolar solutes[41,42] − the hydrophobic effect.[40,43]

In the MB model, the energy of interaction between two waters is

$$U^{ww}(\mathbf{X}_i, \mathbf{X}_j) = U_{LJ}(r_{ij}) + U_{HB}(\mathbf{X}_i, \mathbf{X}_j) \tag{3}$$

The notation is the same as in previous papers: $\mathbf{X}_i$ denotes a vector representing both the coordinates and the orientation of the ith water molecule, and r_{ij} is the distance between the molecular centers of molecules i and j. The LJ term is

$$U_{LJ}(r_{ij}) = 4\epsilon_{LJ}\left[\left(\frac{\sigma_{LJ}}{r_{ij}}\right)^{12} - \left(\frac{\sigma_{LJ}}{r_{ij}}\right)^{6}\right] \tag{4}$$

where ϵ_{LJ} and σ_{LJ} are the well-depth and contact parameters, respectively. In addition, neighboring water molecules form an explicit hydrogen bond when an arm of one water molecule aligns with an arm of another water molecule, with an energy function that is a Gaussian function of separation and angle:

$$U_{HB}(\mathbf{X}_i, \mathbf{X}_j) = \epsilon_{HB} G(r_{ij} - r_{HB}) \sum_{k,l=1}^{3} G(\mathbf{i}_k \cdot \mathbf{u}_{ij} - 1) G(\mathbf{j}_l \cdot \mathbf{u}_{ij} + 1) \tag{5}$$

where $G(x)$ is an unnormalized Gaussian function:

$$G(x) = \exp[-x^2/2\sigma^2] \tag{6}$$

The unit vector $\mathbf{i}_k$ represents the kth arm on the ith particle (k = 1, 2, 3), and $\mathbf{u}_{ij}$ is the unit vector joining the center of molecule i to the center of molecule j (Figure 1a). H-bonding arms are not distinguished as donors or acceptors; only the degree of alignment of two arms determines the strength of a hydrogen bond.

The model parameters are as defined previously.[40] The parameters $\epsilon_{HB} = -1$ and $r_{HB} = 1$ define the optimal hydrogen bond energy and bond length, respectively. The same width parameter $\sigma = 0.085$ is used for both the distance and the angle deviation of a hydrogen bond. The interaction energy in the Lennard-Jones potential function, ϵ_{LJ}, is $^1/_{10}$ of ϵ_{HB}, and the LJ contact distance is 0.7 of that of r_{HB}.[40] Radii for ions are given in units of r_{HB}.

Here, we modified the MB model by including an electrostatic dipole (see Figure 1b). A single negative charge is put at the center of each water molecule, at a distance 0.35 r_{HB} from the surface of the water disk. A single positive charge is put onto one of the H-bonding arms, at a distance 0.165 r_{HB} from the center and 0.185 r_{HB} from the molecule surface. The other two H-bonding arms are uncharged. This position was chosen to match the radius of a Na^+ ion, because sodium ions are found experimentally to cause no change in the entropy of nearby water molecules ($\Delta S_{II} = 0$).[17]

Several other dipole orientations with two or three charges were also tested. However, the model described here was unique in giving qualitatively correct results for water−water liberation free energies and assumed structuring and was used for further analysis.

An ion interacts with the charges on a water molecule through a screened potential:

$$U_{charge} = z_i z_j |\epsilon_{HB}| \alpha \frac{\exp(-\kappa r_{ij})}{r_{ij}} \tag{7}$$

where r_{ij} is the distance between the ion center and a charge on a water dipole, and the valences z_i (z_j) are +1 or −1. All of the distances are in the units of r_{HB}. Various considerations are involved in choosing this functional form. First, while a logarithmic dependence on r is appropriate for a true 2-D system, our model interactions are chosen to be consistent with three-dimensional Coulomb's law. Our model r^{-1} dependence is appropriate for a two-dimensional slice through a three-dimensional system. Second, following others,[44−47] we use a screened Coulomb potential, rather than a simple Coulombic interaction. We use this for computational efficiency. Several groups have shown that when the properties of interest involve only near-neighbor effects, such as those of interest here, the screened Coulomb potential represents an excellent approximation to the Coulomb potential.[48−51] The parameter $\kappa = 0.1$ is small enough that the interaction potential at short distances would not differ substantially from that of a pure Coulombic potential. Decreasing the screening parameter κ did not influence the results.

The last parameter, $\alpha = 2.27$, is chosen so that when a negative ion with a radius 0.35 r_{HB} (the distance of a negative charge from the surface of a water molecule) or a positive ion with a radius 0.185 r_{HB} is in its most favorable position relative to a water molecule, the electrostatic energy equals the hydrogen bond energy ($\epsilon_{HB} = -1$).

The ion−water pair potential is

$$U^{iw}(\mathbf{X}_i, \mathbf{X}_j) = U_{LJ}(r_{ij}) + \sum_{+,-} U_{charge}(\mathbf{X}_i, \mathbf{X}_j) \tag{8}$$

The diameter, σ_{LJ}, is different for different ions ($\sigma_{LJ} = (\sigma_{ion} + \sigma_{water})/2$), while the well depth for the Lennard-Jones potential, ϵ_{LJ}, is taken to be the same for all ions, for simplicity. More realistic models would use different LJ parameters for each ion

(41) Tanford, C. *The Hydrophobic Effect: Formation of Micelles and Biological Membranes*; Wiley: New York, 1980.
(42) Ben-Naim, A. *Hydrophobic Interactions*; Plenum Press: New York, 1983.
(44) Hassan, S. A.; Guarnieri, F.; Mehler, E. L. *J. Phys. Chem. B* **2000**, *104*, 6478−6489.
(45) Ferreira, P. G.; Dymitrowska, M.; Belloni, L. *J. Chem. Phys.* **2000**, *113*, 9849−9862.
(46) Bhattacharya, A.; Mahanti, S. D. *J. Phys.: Condens. Matter* **2001**, *13*, 1413−1428.
(47) Hassan, S. A.; Mehler, E. L. *Int. J. Quantum Chem.* **2001**, *183*, 193−202.
(48) Larsen, B.; Rodge, S. A. *J. Chem. Phys.* **1980**, *72*, 2578−2586.
(49) Rodge, S. A.; Hafskjold, B. *Acta Chem. Scand.* **1981**, *A35*, 263−273.
(50) Leote de Carvalho, R. J. F.; Evans, R. *Mol. Phys.* **1997**, *92*, 211−228.

Table 1. The Crystal Ionic Radii, and Experimentally Obtained Thermodynamics of the Ion Solvation[a]

ion	r_M	hydration number	ΔG^{hyd}	ΔH^{hyd}	ΔS^{hyd}
Li^+	0.060	4.1	−116	−129	−32
Na^+	0.095	5.9	−62	−70	−22
K^+	0.133	7.2	−41	−46	−13
Rb^+	0.148	7.8	−35	−39	−11
Cs^+	0.169	9.6	−26	−29	−8
F^-	0.136	6.4	−73	−80	−24
Cl^-	0.181	7.4	−46	−49	−13
Br^-	0.195	7.2	−44	−47	−11
I^-	0.216	8.1	−34	−36	−7

[a] Shown are the crystal ionic radii, r_M,[55] with the experimentally obtained thermodynamics of the ion solvation: change of Gibbs free energy, ΔG^{hyd}, enthalpy, ΔH^{hyd}, and entropy, ΔS^{hyd}, of hydration[58] per first-shell water molecule. Hydration numbers are taken from ref 60. Ion radii are given in nanometers, ΔG^{hyd} is in units of kJ/mol/hydration number, ΔH^{hyd} is in kJ/mol/hydration number, and ΔS^{hyd} is in J/K/hydration number.

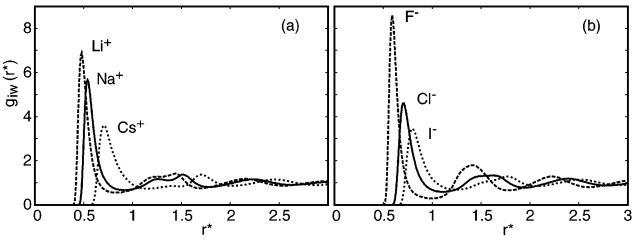

Figure 2. Pair correlation functions of water around ions. (a) Cations and (b) anions. Smaller ions have tighter water shells, at reduced temperature $T^* = 0.20$.

type.[52] While adding such a parameter is likely to improve our agreement with experiments, our aim here is to develop the simplest model for studying ion charge density effects. This model is also simplified in that the dipole on each water molecule interacts only with ions, not with dipoles on other waters. One of the reasons for using the explicit hydrogen bonds versus a dipole−dipole interaction is its quantum mechanical character which is better treated with the "effective" pair potential.[53] Further, the two-dimensional water models using only an electrostatic interaction were unsuitable for describing the anomalous volumetric properties of water.[54]

Ion sizes in our model were taken from crystal ionic radii.[55] The crystal radii are collected in Table 1, and the model ion sizes are collected in Table 2. The relative sizes were calculated from crystal radii. The conversion factor was determined assuming that the negative proportion of the water molecule used by Collins[27] ($r^{neg} = 1.78$ Å) corresponds to the MB-dipole water molecule radius, $\sigma/2 = 0.35\, r_{HB}$. Reduced units are used throughout this paper − all energies and temperatures are normalized to the strength of an optimal hydrogen bond energy (e.g., $T^* = k_BT/|\epsilon_{HB}|$, $U^* = U/|\epsilon_{HB}|$. Similarly, all distances are scaled by the length of an idealized hydrogen bond (e.g., $V^* = V/r_{HB}^2$). We call this the MB-dipole model.

We studied this model through Monte Carlo simulations in the isobaric (NPT) ensemble.[56] A single (positive or negative) ion was fixed in the center of a simulation box. Monte Carlo steps are displacements and rotations of the water molecules; details are given in ref 40. The simulations were usually performed on 120 water molecules. The first 10^7 steps were used to equilibrate the system, and then statistics were collected over the following 5×10^8 steps. Pair distribution functions, $g_{ij}(r)$, and thermodynamic properties (energy, enthalpy, volume) were calculated as ensemble averages.[56] In addition, the free energy, enthalpy, and entropy of transferring an ion or a hydrophobe into a solution were calculated using the Widom test-particle method[57] and using related fluctuation formulas.[40] The results were compared to the molar Gibbs free energy, enthalpy, and entropy of hydration and the standard partial molar volume of ions.[55,58] The experimental values are adjusted to correspond the process of ion transfer into the solution studied here as defined by the Ben−Naim standard state.[58]

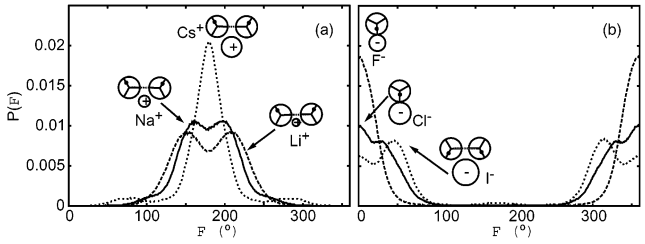

Figure 3. Angular distribution functions for waters in the first shell around an ion, for (a) cations and (b) anions at $T^* = 0.20$. Large cations help promote hydrogen bonding of neighboring waters, leading to a single peak. For small cations, the electrostatic mechanism competes with the hydrogen bond mechanism for ordering waters. The reverse applies to anions. For small anions, the electrostatic mechanism dominates; for large anions, electrostatic and hydrogen-bonding mechanisms compete.

Because Hofmeister effects are linear in ion concentration[8,9] and because anion and cation effects are generally additive and independent,[8,9] we study Hofmeister effects using a water box that contains a single nonpolar solute and a single ion. We performed model hydrophobe transfers (with a disk of the same size as water molecule, $\sigma = 0.7$) from an isolated phase into equilibrated systems of an ion and 60 water molecules. Hofmeister effects in the MB-dipole model were also calculated by examining the potential of mean force (pmf) between an individual ion and a nonpolar solute at infinite dilution, using the Widom method of Shimizu and Chan.[59] The potential of mean force converged to a value near zero at the largest separations measured and did not require other adjustments to attain values near zero.

3. Results: Water Ordering around Ions

First, we studied the structure of MB-dipole water around ions. Figure 2a and b shows the ion−water pair distribution functions for cations and anions of different sizes. The sizes represent very small (Li^+, F^-), intermediate (Na^+, Cl^-), and large (Cs^+, I^-) ions. These figures show that the smaller ions are bound more closely to water molecules than are larger ions.

Figure 3 shows the angular distributions of first-shell waters around ions. The angle is of a water's dipole vector relative to the vector connecting the water and ion centers. The favored angle is $\theta = 0$ for a water molecule adjacent to an anion, because water points the positive end of its dipole directly at the anion (see Figure 3b). The favored angle is $\theta = 180°$ for a water

(52) Hummer, G.; Pratt, L. R.; Garcia, A. E. *J. Phys. Chem.* **1996**, *100*, 1206−1215.
(53) Ben-Naim, A. *Water and Aqueous Solutions*; Plenum Press: New York, 1974.
(54) Okazaki, K. *J. Chem. Phys.* **1981**, *75*, 5874−5884.
(55) Marcus, Y. *Ion Solvation*; Wiley-Interscience: New York, 1985.
(56) Allen, M. P.; Tildesley, D. J. *Computer Simulation of Liquids*; Oxford
(57) Widom, B. *J. Chem. Phys.* **1963**, *39*, 2808−2812.
(58) Marcus, Y. *Biophys. Chem.* **1994**, *51*, 111−127.

Table 2. Ion Diameters Used in the MB-Dipole Model, and Ion Insertion Thermodynamics into MB-Dipole Water[a]

ion	σ	hydration number	ΔG^{hyd}	ΔH^{hyd}	ΔS^{hyd}	E^{el}
Li^+	0.24	3.29	-16.01 ± 0.04	-30.2 ± 0.2	-24.2 ± 0.3	-28.59 ± 0.07
Na^+	0.37	3.50	-12.09 ± 0.06	-24.7 ± 0.3	-21.6 ± 0.5	-23.25 ± 0.07
K^+	0.52	4.01	-8.22 ± 0.03	-19.4 ± 0.4	-19.1 ± 0.6	-17.8 ± 0.1
Rb^+	0.58	4.38	-6.82 ± 0.03	-17.5 ± 0.4	-18.2 ± 0.8	
Cs^+	0.66	4.53	-5.78 ± 0.03	-16.5 ± 0.5	-18.2 ± 0.7	-14.25 ± 0.05
F^-	0.53	4.12	-14.1 ± 0.1	-25 ± 3	-18 ± 4	-31.9 ± 0.1
Cl^-	0.71	4.35	-7.78 ± 0.08	-16 ± 2	-13 ± 4	-18.99 ± 0.06
Br^-	0.77	4.55	-6.4 ± 0.1	-13 ± 1	-11 ± 2	-16.28 ± 0.05
I^-	0.85	4.83	-4.62 ± 0.03	-10.8 ± 0.4	-10.5 ± 0.7	-13.5 ± 0.1

[a] Shown are ion diameters used in the MB-dipole model, σ, and the change in Gibbs free energy, ΔG^{hyd}, enthalpy, ΔH^{hyd}, entropy, ΔS^{hyd}, and electrostatic energy, ΔE^{el}, per first-shell water molecule, for ion insertion in MB-dipole water, as obtained from the Widom insertion method at $T^* = 0.20$. Ion radii are given in reduced units for the MB-dipole model. ΔG^{hyd}, ΔH^{hyd}, and ΔS^{hyd} have the same units as in Table 11, assuming ϵ_{HB} in the MB-dipole model has an energy of 24.37 kJ/mol.[53]

molecule adjacent to a cation, because water points the positive end of its dipole directly away from the ion (Figure 3a). Figure 3 shows that first-shell waters around an ion are highly oriented, dominated by these preferred orientations.

Figure 3 shows that water orientations result from a balance between this electrostatic ordering mechanism and the water−water hydrogen-bonding ordering mechanism. For the smallest anions (F^- and Cl^-), the electrostatic mechanism dominates: water molecules orient to achieve the most favorable electrostatic orientation with respect to the ion. This is supported by all-atom classical force-field studies of anions in small clusters of water.[60−64] Yet for larger anions (I^-), the first-shell water orientational distribution has two peaks. In that case, water's orientation is a compromise between the electrostatic tendency to orient the dipole with respect to the ion and the hydrogen-bonding tendency to orient two adjacent water molecules in the ion's first shell.

The same balance applies to cations, except that the size tendency is reversed. Figure 3a shows that the large cations (Cs^+) cause a single-peaked and narrow angular distribution of water because the electrostatic tendency is compatible with the hydrogen-bonding tendency in this case. In contrast, the smaller cations lead to double-peaked distributions, implying that the water−water hydrogen bonds are "bending" the dipole angles. Such configurations are also seen in all-atom calculations of intermediate size cation−water cluster structures.[65−68] The exception is the Li^+ water cluster structure[69] which will be discussed in more detail below.

Figure 4 shows the average number of hydrogen bonds made by a water molecule within the first water shell around an ion. This quantity shows the balance between electrostatics and hydrogen bonding. It shows that for the large cations, electrostatics *assists* in the formation of water−water hydrogen bonds, while for all other ions, electrostatics *competes against* hydrogen bond formation. The ions having the highest charge densities

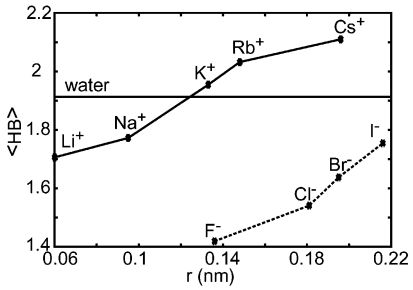

Figure 4. The average number of the water−water hydrogen bonds, ⟨HB⟩, per water molecule in the first shell around various ions at $T^* = 0.20$.

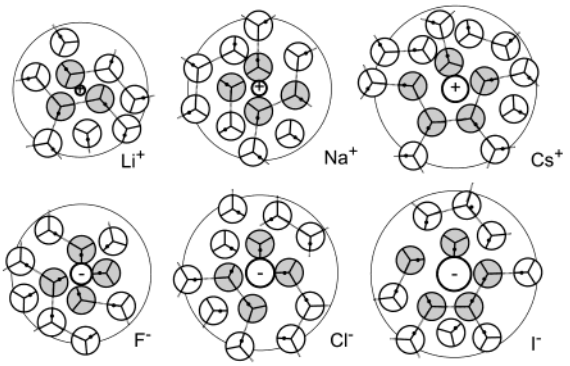

Figure 5. Snapshots of waters in the first (shaded) and second shell (white) around an ion (black), showing likely configurations of water as inferred from statistics of pair distributions, angular orientations, and hydrogen bonding at $T^* = 0.20$.

(F^-, for example) are the most disruptive of water−water hydrogen bonding. All-atom ion−water simulations show overall breaking of hydrogen bonds (relative to bulk water) in small clusters around ions with high charge density.[70,71] However, in contrast to our MB-dipole model results, hydrogen bond formation is more probable between water molecules clustered around anions than around cations.[71]

Figure 5 summarizes these results. Small cations orient first-shell waters through an electrostatic mechanism, disrupting hydrogen bonding among first-shell waters. Increasing the cation size diminishes the electrostatic force of the ion on the water, leading to increased water−water hydrogen bonding, as would be seen around nonpolar solutes. A similar trend occurs for anions: water structure around small anions is controlled by

(60) Lee, S. H.; Rasaiah, J. C. *J. Phys. Chem.* **1996**, *100*, 1420−1425.
(61) Xantheas, S. S.; Dang, L. X. *J. Phys. Chem.* **1996**, *100*, 3989−3995.
(62) Bryce, R. A.; Vincent, M. A.; Malcolm, N. O. J.; Hillier, I. H. *J. Chem. Phys.* **1998**, *109*, 3077−3085.
(63) Sremaniak, L. S.; Perera, L.; Berkowitz, M. L. *J. Phys. Chem.* **1996**, *100*, 1350−1356.
(64) Ayala, R.; Martinez, J. M.; Pappalardo, R. R.; Marcos, E. S. *J. Phys. Chem. A* **2000**, *104*, 2799−2807.
(65) Kollman, P. A.; Kuntz, I. D. *J. Am. Chem. Soc.* **1972**, *94*, 9236−9237.
(66) Kollman, P. A.; Lybrand, T.; Cieplak, P. *J. Chem. Phys.* **1988**, *88*, 8017.
(67) Caldwell, J. W.; Kollman, P. A. *J. Phys. Chem.* **1992**, *96*, 8249−8251.
(68) Ramaniah, L. M.; Bernasconi, M.; Parinello, M. *J. Chem. Phys.* **1999**, *111*, 1587−1591.
(69) Lyubartsev, A. P.; Laasonen, K.; Laaksonen, A. *J. Chem. Phys.* **2001**, *114*,
(70) Combariza, J. E.; Kestner, N. R. *J. Phys. Chem.* **1995**, *99*, 2717−2723.
(71) Topol, I. A.; Tawa, G. J.; Burt, S. K.; Rashin, A. A. *J. Chem. Phys.* **1999**,

DOCKET ALARM

Explore Litigation Insights

Docket Alarm provides insights to develop a more informed litigation strategy and the peace of mind of knowing you're on top of things.

Real-Time Litigation Alerts

Keep your litigation team up-to-date with **real-time alerts** and advanced team management tools built for the enterprise, all while greatly reducing PACER spend.

Our comprehensive service means we can handle Federal, State, and Administrative courts across the country.

Advanced Docket Research

With over 230 million records, Docket Alarm's cloud-native docket research platform finds what other services can't. Coverage includes Federal, State, plus PTAB, TTAB, ITC and NLRB decisions, all in one place.

Identify arguments that have been successful in the past with full text, pinpoint searching. Link to case law cited within any court document via Fastcase.

Analytics At Your Fingertips

Learn what happened the last time a particular judge, opposing counsel or company faced cases similar to yours.

Advanced out-of-the-box PTAB and TTAB analytics are always at your fingertips.

API

Docket Alarm offers a powerful API (application programming interface) to developers that want to integrate case filings into their apps.

LAW FIRMS
Build custom dashboards for your attorneys and clients with live data direct from the court.

Automate many repetitive legal tasks like conflict checks, document management, and marketing.

FINANCIAL INSTITUTIONS
Litigation and bankruptcy checks for companies and debtors.

E-DISCOVERY AND LEGAL VENDORS
Sync your system to PACER to automate legal marketing.